

Using Geant4 to create 3D maps of dosage received within a MinPET diamond sorting facility

MNH Cook and SH Connell

University of Johannesburg, Johannesburg, South Africa

E-mail: martin@minpet.co.za

Abstract. The MinPET project aims to locate diamonds within kimberlite by activating carbon within kimberlite, then using Positron Emission Tomography (PET) to image carbon density. Although calculations suggest that long-term activation is not significant, modelling is required to determine the dose received by workers operating close to recently activated material at different positions within a hypothetical MinPET sorting unit. Two modelling techniques are deployed to investigate received dose. The first is a full simulation of energy absorbed, using the CERN Geant4 particle tracking toolkit. The results for this are validated against a numerical computation of the attenuation of outgoing radiation. The result is a set of 3-dimensional dosage maps. These can be used to set guidelines around where and for how long workers could operate, and to identify areas that need additional radiation shielding. The techniques developed are not limited to MinPET, and could prove useful for any situation requiring the simulation of dose received by workers operating near radioactive material.

1. Introduction

The MinPET project [1] images locked diamonds within coarsely crushed kimberlite (± 10 cm rocks), using Positron Emission Tomography (PET). The kimberlite is irradiated with high energy gamma rays, producing the unstable ^{11}C isotope via a photonuclear reaction. This beta decays, and the positron annihilation leads to back-to-back collinear 511 keV photons. These are detected in coincidence by two planes of position sensitive detectors above and below the kimberlite. A 3D carbon density image is created by back-projecting the lines of response. Because the signal from oxygen-15 (with a 2 minute half-life) dominates early on, irradiated material is held for 20-30 minutes before it goes to the detectors. At this point, the carbon-11 starts to dominate, due to its longer 20 minute half-life.

One of the concerns for an industrial scale MinPET plant is the radiation exposure of workers. The shielding requirements for the irradiation system have already been investigated in [2]. This included radiation shielding calculations, analysis, and optimisation with the aid of the MCNPX Monte Carlo code. The conclusion was that a 1.6 m thick shielding matrix of lead, iron, wax and boron carbide adequately shielded personnel from the irradiation system. If the accelerator, irradiation system and hold hopper were buried underground away from personnel, these requirements would be less stringent. The hold hoppers where kimberlite is stored can also be shielded.

It therefore remains to quantify the radiation hazard posed by activated material after the 20-30 minute point. Two scenarios we are especially interested in understanding are the dose received by workers near the conveyor belt at time of detection, and near a discarded pile of mine

tailings. Two numerical techniques have been developed to calculate the exposure given by a particular geometry of radioactive material. The first uses an attenuation model to arrive at an integral that can be solved numerically. This technique only applies to rectangular cuboid bodies of material. The results of this are compared to a full Monte Carlo physics simulation that is more accurate, but far more computationally intensive. The second technique can, however, be applied to any geometry.

2. MinPET Activity Levels

A series of irradiations were performed at the 100 MeV electron accelerator at Aarhus University [3]. These identified two isotopes that are of concern over time scales greater than 20 minutes, namely carbon-11 and sodium-24.

Assuming a 0.2% CO₂ concentration in kimberlite, at run-of-mine MinPET specifications (feed rate of 700 tons/hour and 1s irradiation with a 1m² footprint photon beam from a 40 MeV optimally converted electron bremsstrahlung beam [4]), the combined oxygen and carbon activity is 33.9 Bq/g at the 29 minute mark. Each beta decay leads to two positron annihilation photons, so this is equivalent to a photon rate of 67.8 Hz/g. The measured sodium-24 concentration in our Aarhus sample, extrapolated to MinPET conditions, was 1.01 Bq/g.

3. Attenuation Model

3.1. General Case

The intensity of a mono-energetic photon beam passing through a material can be described using a linear attenuation constant, μ_L , as follows:

$$\frac{I}{I_0} = e^{-\mu_L x} \quad (1)$$

This does not capture the full story however, as once a photon interacts with an atom, all of its energy does not always disappear into the medium. Photons interact with the medium predominantly via pair production, the photoelectric effect and Compton scattering [5]. These can leave the primary photon with some energy, and can also release charged particles which are then free to interact further. One way of quantifying this is with a mass energy-absorption coefficient μ_{en} (see, for example, [6]). This attempts to quantify the energy absorbed by a material through which photons are passing. If, at each step dx , the material absorbs an energy dE given by $dE = E\mu_{en}dx$, then the energy that is not yet absorbed follows an exponential decay of the form of equation (1). We shall refer to the attenuation constant simply as μ , which is a function of both the photon energy and the material being traversed.

Given the specific activity S_A (presumed measured in Bq.m⁻³) of a radioactive isotope, and a photon energy E_γ , our goal is to find the overall energy incident on an object near some radioactive material per unit time. This will allow a radiological assessment of risk, to a person, in the proximity of the source. Using equation (1), the energy incident per unit time (dP) on a small surface area centred at point Q due to a small volume element dV centred at point P is

$$dP = \frac{d\Omega(P, Q)}{4\pi} dV S_A E_\gamma e^{-\mu l(P, Q)} \quad (2)$$

where $d\Omega$ is the solid angle subtended by the small area and l is the path length travelled by the radiation through the material. To find the total power incident on a target, we integrate over the volume of radioactive material, and over the solid angle subtended by the object. If the target is small or far away, then l does not change much for different points on the target, and $l(P, Q) \approx l(P)$. The integral over $d\Omega$ collapses to the total solid angle subtended by the target, Ω . We further simplify by considering a spherical target of radius r . The solid angle subtended

by a sphere is $\Omega = 2\pi(1 - \sqrt{1 - r^2/R^2})$, where R is the distance to the sphere, and thus the total power incident on the target due to a volume V is

$$P = \frac{S_A E_\gamma}{2} \int_V dV \left(1 - \sqrt{1 - \frac{r^2}{R^2}} \right) e^{-\mu l} \quad (3)$$

3.2. Rectangular Cuboid Volume

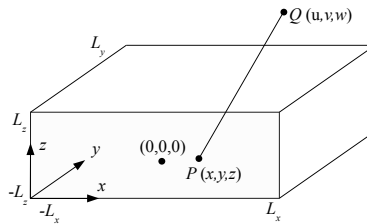


Figure 1. Rectangular geometry in attenuation model

In the case of a cuboid volume, with coordinates as shown in figure 1, the path length l can be expressed in terms of R : $l = R \left(\frac{L_z - z}{w - z} \right)$. The power will now be given by

$$P = \frac{S_A E_\gamma}{2} \int_{-L_x}^{L_x} dx \int_{-L_y}^{L_y} dy \int_{-L_z}^{L_z} dz \left(1 - \sqrt{1 - r^2/R^2} \right) e^{-\mu \left(\frac{L_z - z}{w - z} \right) R} \quad (4)$$

where $R^2 = (x - u)^2 + (y - v)^2 + (z - w)^2$. This integral does not have a readily available analytic solution and is calculated numerically.

An additional complication arises because equation (4) assumes that the photons passes through the upper z face. In the general case, an extra step is required at each point of the integral, that tests which face of the cuboid is intersected by the line joining P and Q . The coordinates of the term in the exponential can then be rotated appropriately.

4. Monte Carlo Simulation

In order to get results in more complex geometries, a full simulation is needed to individually track particles from emission to target impact. The toolkit of choice is the Geant4 framework [7][8], created at CERN.

In order to compare results to the attenuation model, we first find the effective energy attenuation within kimberlite of Geant4 simulations. Photons are fired out from the centre of a large sphere, and the energy that makes it to a certain radius is graphed against the radius. This is fitted with an exponential decay in figure 2. 511 keV and 1369 keV are the energy levels from the PET isotopes and sodium respectively. 100 keV was included as a lower energy comparison. The fit is relatively good, with only small divergences at high and low energy. This validates the treatment of energy loss with a simple exponential attenuation. From the slope of the exponential fits in figure 2, the effective Geant4 energy attenuation constants are $9.352 \pm 0.002 \text{ m}^{-1}$ for 1369 keV, $12.804 \pm 0.004 \text{ m}^{-1}$ for 511 keV and $26.37 \pm 0.02 \text{ m}^{-1}$ for 100 keV.

The full Geant4 simulation consists of an activated kimberlite volume and a human phantom (sphere of water that makes up the target). We will use a water sphere of radius 0.5 m. This has the same frontal surface area as a standing person, approximated as 1.7 m tall and 50 cm wide. If more accuracy is desired, a more realistic shape can easily be created, but the advantage of a sphere is that the results are directly comparable to those from the attenuation model, for cross-checking. The sphere is placed at a succession of positions on a three dimensional grid.

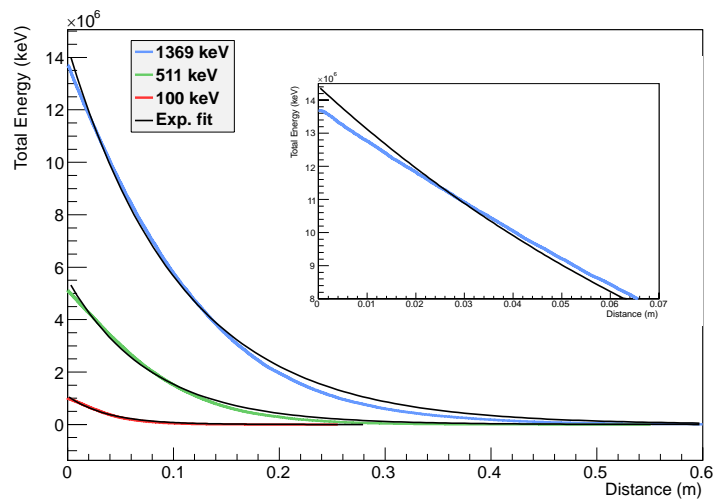


Figure 2. Difference between Geant4 simulation and simple attenuation model. Coloured lines show simulated data from Geant4. Inset shows magnification of lower radius region for 1369 keV.

5. Results

5.1. Comparison between Attenuation Model and Geant4 Simulation

An example geometry was created with a kimberlite cuboid 2 m high, 4 m wide and 6 m long. A 0.5 m radius spherical target was then moved along a horizontal plane at a height of 0.6 m above the cuboid, and the energy deposited was calculated using both the attenuation model and the Geant4 simulation. The attenuation model was integrated numerically using the Vegas algorithm from ROOT [9]. The Geant4 simulation fired 1 000 000 particles for each data point and recorded the energy that hit the target. The results are shown in figure 3. The agreement is quite good. The major qualitative difference is that the Geant4 simulation is not as smooth, as it is a stochastic Monte Carlo simulation.

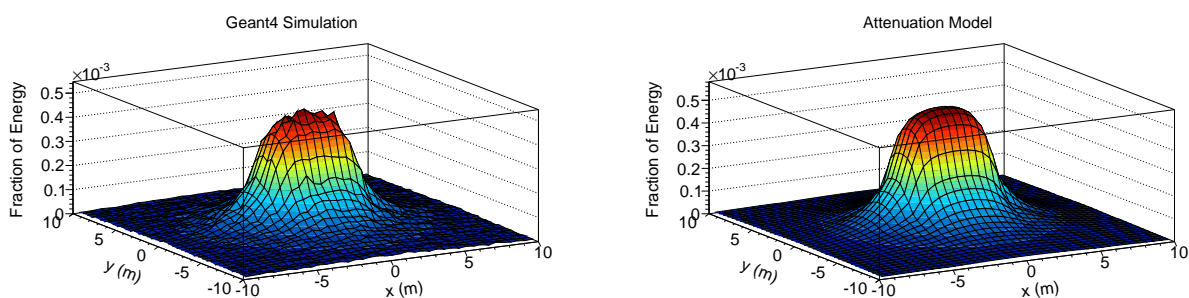


Figure 3. Fraction of activity reaching target in Geant4 simulation and attenuation models.

Small non-statistical differences between the models are observed at small distances. This is to be expected, because the derivation of equation 3 relied on the assumption that the target is small compared to the distance between the target and the source.

5.2. Kimberlite on Belt

We now investigate a body of material moving on a conveyor belt at the time of detection. The kimberlite can be approximated as a rectangular cuboid of material, and is therefore a candidate for the numerical integral technique. We will consider a 20 m long kimberlite stream, 1 m wide and 10 cm tall, using the 67.8 Hz/g photon rate from section 2. We assume a packing density of 0.7 for kimberlite, which is approximated by using kimberlite which is 30% air by volume.

Figure 4 shows the activity absorbed by the target as a function of the position of the centre of the target. The conveyor belt extends from $x = -10$ m to $x = 10$ m, and from $y = -0.5$ m to $y = 0.5$ m. The edge of the target is 5 cm from the belt at its closest, and the centre of the target is 30 cm above the belt. This approximates a worker standing at various positions next to the conveyor belt. Both the activity in Bq/cm^3 and the gamma attenuation constant are multiplied by 0.7 to take the packing density into account.

The activity that hits the target when there is a 5 cm horizontal gap between the belt and the target, i.e. a 105 cm horizontal distance between centre of belt and centre of target, is 2.40×10^5 photons/s. Considering a photon energy of 511 keV and a gamma radiation quality factor of 1 [5], this corresponds to $70.8 \mu\text{Sv}/\text{h}$. At a distance of 1 m, this has already fallen to 7.50×10^4 photons/s or $22.1 \mu\text{Sv}/\text{h}$. Workers would have to spend six hours a day for 118 days at a distance of 5 cm, to reach the 50 mSv level set in the IAEA safety guide relating to radioactive material in mining [10]. Workers could be employed full time at a distance of 1 m. The kimberlite will be more active at the time of detection if the carbon dioxide concentration is substantially greater than 0.2%. In this case, worker access should be more limited. It is not anticipated that workers would need to spend significant time periods at the side of the belt.

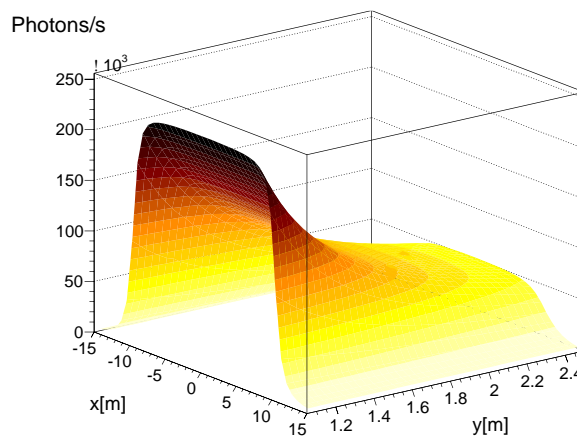


Figure 4. Activity at different points along the side of a $20 \text{ m} \times 1 \text{ m}$ conveyor belt carrying kimberlite 10 cm deep. Positions quoted are for the centre of a water target, relative to the centre of the belt.

5.3. Tailings

To reproduce a pile of tailings, a Geant4 simulation of a trapezoid was made, with a base side length of 6 m and a top diameter of 4 m, 2 m high. Only the ^{24}Na was considered, as all other isotopes have died away when several hours have passed. We use the worst case scenario of 1.01 Bq/g. Again, we model a 0.7 packing density by simulating kimberlite with 30% air content, and multiplying the activity per cm^3 by 0.7.

According to the Geant4 simulation, the fraction of the energy that reaches the target is 2.72×10^{-4} . This means that 24 hours after irradiation, the target receives an energy dose of

6.54×10^{-8} J/s, taking into account the fact that sodium decays are associated with the release of gamma rays at three different energies, 472 keV, 1369 keV and 2754 keV. This is equivalent to about $23.5 \mu\text{Sv/h}$. After 72 hours, this has dropped to $2.55 \mu\text{Sv/h}$. According to the ALARA principle of as little exposure as possible, preferably humans should not be too close to the tailings during the first day. A worker could, however, work full time near a one day old 6 m wide tailings pile and not exceed the IAEA guidelines for one year exposure.

6. Conclusions

We have explored two techniques for finding position specific radiation exposures due to specific geometries of radioactive material. The results for each are in close correspondence. The attenuation model is quick to calculate, and is useful for simple geometries such as cuboids. Calculating the graph shown took seconds on a personal computer. The Geant4 simulation is far more powerful, as it can simulate any geometry, and can easily be extended to include layers of shielding etc. The downside is that it is far more computationally intensive. A single (x, y) point from figure 3, with one million events, took 5 minutes to compute on a personal computer. The University of Johannesburg's cluster computer [11] was therefore used to generate the graph of activity as a function of position.

In both scenarios considered, it is clear that the radiation dose levels to workers in a MinPET plant would be acceptable, in the context of a well-controlled radiation producing facility.

References

- [1] Ballestrero S, Bornman F, Cafferty L, Caveney R, Connell S, Cook M, Dalton M, Gopal H, Ives N, Lee C A, Mampe W, Phoku M, Roodt A, Sibande W, Sellschop J P F, Topkin J and Unwucholaa D A 2010 Mineral-PET: Kimberlite sorting by nuclear-medical technology *12th International Conference on Nuclear Reaction Mechanisms* ed Cerutti F and Ferrari A (Varenna, Italy) pp 589–602
- [2] Chinaka E M, Zibi Z, van Rooyen J, Connell S H and Cook M *To appear in the these conference proceedings of the 2016 South African Institute of Physics Conference*
- [3] Tchonang M, Cook M, Bornman F, Connell S and Ballestrero S 2013 Elemental Analysis of Kimberlite and Associated Country Rock *Proceedings, 58th Annual Conference of the South African Institute of Physics (SAIP 2013)* ed Botha R and Jili T pp 502–506 ISBN 9780620628198 URL <http://events.saip.org.za/getFile.py/access?resId=0&materialId=9&confId=32>
- [4] Cook M 2014 *Remote Detection of Light Elements Using Positron Emission Tomography* (PhD Thesis : University of Johannesburg)
- [5] Leo W 1994 *Techniques for Nuclear and Particle Physics Experiments: A How-to Approach* (Springer) ISBN 9783540572800 URL <http://books.google.co.za/books?id=hDEbAQAIAAJ>
- [6] Seltzer S 1993 *Rad. Res.* **136** 141–70
- [7] Agostinelli S *et al.* 2003 *Nuclear Instruments and Methods A* **506** 250–303
- [8] Allison J, Amako K, Apostolakis J, Araujo H, Dubois P *et al.* 2006 *IEEE Trans.Nucl.Sci.* **53** 270–8
- [9] Brun R and Rademakers F 1997 *Proceedings AIHENP'96 Workshop, Lausanne, Sep. 1996, Nucl. Inst. & Meth. in Phys. Res. A* **389** 81–86 see also <http://root.cern.ch/>.
- [10] International Atomic Energy Agency 2002 Management of radioactive waste from the mining and milling of ores series No. WS-G-1.2
- [11] University of Johannesburg cluster. URL <http://physics.uj.ac.za/clusters>